Available online at www.sciencedirect.com
ScienceDirect
International Journal of Fatigue 28 (2006) 1739–1751
International Journal of Fatigue
www.elsevier.com/locate/ijfatigue

Practical fatigue analysis of hydraulic cylinders and some design recommendations

I. Marczewska [a], T. Bednarek [a], A. Marczewski [a,*], W. Sosnowski [a], H. Jakubczak [b], J. Rojek [a]

[a] Institute of Fundamental Technological Research, Polish Academy of Science, ul. Swietokrzyska 21, 00-049 Warsaw, Poland
[b] Warsaw University of Technology, Faculty of Automotive and Construction Machinery Engineering, Institute of Construction Machinery Engineering, ul. Narbutta 84, 02-524 Warsaw, Poland

Received 7 July 2005; received in revised form 21 November 2005; accepted 4 January 2006
Available online 7 March 2006

Abstract

In this paper, a numerical algorithm is presented which makes it possible to adopt the different loading schemes of specific structure at hand, for instance hydraulic cylinders, to specific Wöhler curves characterizing fatigue resistance of the given material. The model used in this paper is based on particular application of the constitutive model described in reference [S. Oller, O. Salomon, E. Onate, A continuum mechanics model for mechanical fatigue analysis, Comput Mater Science 2005;32(2):175–95]. Hydraulic cylinders investigated under E.C. project "PROHIPP" are analyzed and some solution of the crack problem in oil port area is proposed. Calculations have to be done for cylinders under loads, which differ from the experimental data provided in Wöhler curve. Oil penetration in oil port connection zone can be eliminated after some design modifications. As it is written at the end of EN 13445 rules description (point 18I) [European Norm EN 13445. Unifired pressure vessels, chapter 18: Detailed assessment of fatigue life, http://www.unm.fr/en/general/en13445/default.htm], the 'marriage' of stress analysis from finite element analysis and fatigue data is still one of the deficiencies in the current EN 13445. We believe that this paper partially reduces this deficiency.

Keywords: Endurance limit; Hydraulic cylinders; Wöhler curves; Goodman diagrams

1. Introduction

There are two objectives of this paper. The first objective is to present a numerical algorithm which makes it possible to adopt different loading schemes of hydraulic cylinders to specific Wöhler curves characterizing fatigue resistance of the given material. Uniaxial loading case is studied in order to find out the relation between Goodman and Wöhler curves parameters. The second target is to present calculations of hydraulic cylinders investigated under E.C. project "PROHIPP" and to propose some solution of the crack problem in oil port area, in order to eliminate oil penetration in oil port connection zone. The model used in this paper is based on particular application of the constitutive model described in Ref. [1].

It is well known that majority of the fatigue test are made for symmetric or nearly symmetric load, when

$$R = \frac{p_{\min}}{p_{\max}} = \frac{S_{\min}}{S_{\max}} = -1. \quad (1)$$

The number of codes accept input data only for such kind of symmetric load. In practice majority of structures, for instance hydraulic cylinders, work under much more complex cyclic load characterized by different R values. In particular, typical laboratory tests are performed for $R = 0$, when the stresses change from 0 to some specific, maximal value. This is the case of the hydraulic cylinders, tested usually in such a way, where external pressure is applied to the

* Corresponding author. Tel.: +22 8261281x147; fax: +48 22 8269815.
E-mail address: asmar@ippt.gov.pl (A. Marczewski).

0142-1123/$ - see front matter © 2006 Elsevier Ltd. All rights reserved.
doi:10.1016/j.ijfatigue.2006.01.003

cylinder and then the pressure is removed. The equivalent amplitude stress is introduced in order to find out the number of cycles to failure for load with mean stress ratio $R \neq -1$ (see Eq. (1)) in situations, when experimental test data (Wöhler curve) are provided only for values $R = -1$.

The number of cycles in such tests depends on fatigue resistance of the weakest point of the cylinder. An example of such points is oil ports, where the welding residual stresses, local shear forces and forces due to oil penetration in the connection gaps lead to fatigue cracks causing final destruction.

Two kinds of numerical tests are performed. First, the standard fatigue tests on workpiece which are shown in Fig. 5 are simulated (Section 3). Typical material characteristics are used in order to generate proper Wöhler curve for two different load schemes: symmetric load with $R = -1$ and unsymmetric load for $R = 0$. Goodman curves and classical Wöhler curves are used in order to calculate the number of cycles to reach the fatigue limit.

Next, in Section 4, the hydraulic cylinders fatigue problem is considered. Oil port typical deformations and the possible design modifications are shown in Fig. 16. It can be observed that the gap between the oil port and the cylinder in the oil port connection zone increases with increasing oil pressure. Also, experiments (Fig. 16) confirm the crack sensitivity of the weld in this connection zone. The authors propose the improvement of this bad situation by using special *washer* or *glue* in order to eliminate excessive gap between oil port and cylinder surfaces. Such washer or glue prevents oil penetration, thus eliminating the possibility of premature fatigue crack in neighboring welds.

The washer or glue material should be high temperature resistant – due to welding process of oil ports.

In the whole paper, the stress fields calculated by 3D FEM structure models are represented by 1D ultimate von Mises stress calculated from formula

$$S_{\max} = \sqrt{S_x^2 + S_y^2 + S_z^2 - S_x S_y - S_y S_z - S_z S_x + 3(S_{xy}^2 + S_{yz}^2 + S_{zx}^2)}$$

in order to be used in 1D fatigue analysis. Components S_x, S_y, S_z are the stress values in the given x, y and z directions. S_{xy}, S_{yz}, S_{zx} are the shear stresses.

2. Wöhler and Goodman curves dependency

The history of standard fatigue test goes back to Wöhler who designed and built the first rotating-beam test machine that produced fluctuating stress of a constant amplitude in test specimens [3,4]. In these tests, Wöhler established a material property, known today as the *fatigue limit*, $S^{\mathrm{at}}_{(R)}$ (threshold stress). Where specific fatigue data are missing, for example the number of cycles to failure for the given stress ratio, one can use empirical correlation between stress and fatigue life N as linear approximation of the S–N curve in log–log coordinates. Wöhler curve as a function of N cycles which is shown in Fig. 1 is obtained by

$$S^{\mathrm{a}}(N) = 10^{\frac{\log(S^{\mathrm{at}}_{(R)}) - \log(S^{\mathrm{ai}}_{(R)})}{\log(N_{\mathrm{t}}) - \log(N_{\mathrm{i}})}\log(N) - \left(\log(N_{\mathrm{i}})\frac{\log\left(S^{\mathrm{at}}_{(R)}\right) - \log\left(S^{\mathrm{ai}}_{(R)}\right)}{\log(N_{\mathrm{t}}) - \log(N_{\mathrm{i}})} + \log\left(S^{\mathrm{at}}_{(R)}\right)\right)}, \tag{2}$$

where $N_{\mathrm{i}} = 1.0 \times 10^3$ and $N_{\mathrm{t}} = 2.0 \times 10^6$. Initial amplitude stress $S^{\mathrm{ai}}_{(R=-1)}$ for $N_{\mathrm{i}} = 1.0 \times 10^3$ (initial number of cycles) can be obtained from

$$S^{\mathrm{ai}}_{(R=-1)} = S_{\mathrm{u}} \cdot f^i, \tag{3}$$

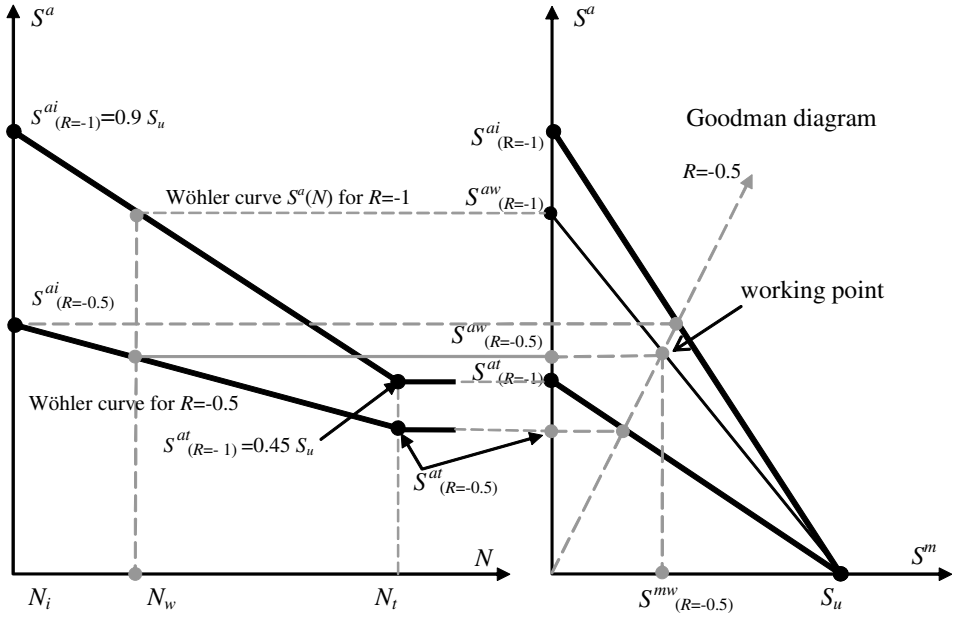

Fig. 1. Wöhler and Goodman diagrams dependency.

where f^i is decreasing factor of stress corresponding to $N_i = 1.0 \times 10^3$ cycles. The value of f^i can be found in the literature [1,3,5,6]. In this paper i is equal to 0.9. The value of threshold amplitude stress $S^{at}_{(R=-1)}$ for $N_t = 2.0 \times 10^6$ (threshold number of cycles) is obtained by

$$S^{at}_{(R=-1)} = S_u \cdot f^t, \tag{4}$$

where f^t is the decreasing factor of stress corresponding to stress threshold value. The value of f^t changes between 0.05 and 0.5 and depends on material properties and stress concentration factor [1,3,5,6]. In this paper t is equal to 0.45.

Substituting $S^a(N) = S^{aw}_{(R)}$, where index w means the working point, and transforming Eq. (2) we can obtain the number of cycles to failure N_w for a given amplitude stress S^{aw}

$$N_w = 10^{\frac{\log(S^{aw}_{(R)})\log(N_i) - \log(S^{aw}_{(R)})\log(N_t) + \log(S^{ai}_{(R)})\log(N_t) - \log(S^{at}_{(R)})\log(N_i)}{\log(S^{ai}_{(R)}) - \log\left(S^{at}_{(R)}\right)}}. \tag{5}$$

where the standard S–N (Wöhler) curve (see Fig. 1, left) is based on amplitude stress, $S = S^a$ or maximal stress $S = S^{max}$.

Usually, Wöhler curve is obtained for fully reversed stress ($R = -1$) by rotating bending fatigue tests or axial-load test ($R = 0$). However, this zero or -1 mean ratio stress is not typical for real industrial components working under cyclic load.

Based on the value of ultimate stress S_u and the value of amplitude stress $S^a_{R\neq -1}$, we can obtain the value of the amplitude stress $S^a_{R=-1}$ from Goodman diagram (see Fig. 1, right).

Goodman line is represented by the linear equation

$$S^a = S^{at}_{(R=-1)}\left(1 - \left(\frac{S^m}{S_u}\right)\right). \tag{6}$$

If the value of the mean stress S^m is equal to 0 (for $R = -1$), then we get $S^a = S^{at}_{(R=-1)}$. Values of the mean stress S^m are obtained from

$$S^m = \frac{S^a(1+R)}{(1-R)}. \tag{7}$$

Amplitude of stress for $R = -1$ is obtained from Eq. (6)

$$S^{at}_{(R=-1)} = \frac{S^a}{\left(1 - \left(\frac{S^m}{S_u}\right)\right)}. \tag{8}$$

The value of the amplitude stress calculated from Eq. (8) can be next substituted into Eq. (5), where $S^{at}_{(R)} \equiv S^{at}_{(R=-1)}$, in order to calculate the number of cycles to failure of analyzed structure loaded by arbitrary, non-symmetric load with any stress ratio $R \neq -1$.

2.1. Influence of arbitrary chosen parameter R on behavior of the S-N function

The Wöhler curve can be expressed as the relation between the amplitude stress S^a versus the number of cycles to failure N in log–log scale. Different way of introducing the Wöhler curve is to express it as the relation between the maximal stress S^{max} versus the number of cycles to failure N. S^{max} and S^a are used next in Section 5 in final calculation of the number of cycles N to failure. Two ways of calculating $S^{max}_{(R)}$ will be presented. The equation for constructing the Wöhler curve $S^{max}_{(R)}(N)$ in dependency from $S^{max}_{(R)}$ will be presented below.

The maximal value of stress for different values of R which we obtain from dependency is

$$S^{max}_{(R)} = S^a_{(R)} + S^m_{(R)}, \tag{9}$$

where $S^a_{(R)}$ is the amplitude stress for different values of R given by:

$$S^a_{(R\neq -1)} = \frac{S_u S^a_{(R=-1)}(R-1)}{S^a_{(R=-1)}(-1-R) + S_u(R-1)} \tag{10}$$

which is obtained by expressing S^m as function S^a and R (see Eq. (6)).

The maximal stress $S^{max}_{(R)}$ for arbitrary value of R can also be obtained from

$$S^{max}_{(R)} = S^{at}_{(R=-1)} + \left(S_u - S^{at}_{(R=-1)}\right) \cdot (0.5 + 0.5 \cdot R)^{STHR1} \tag{11}$$

given in paper [1]. $STHR1$ is a parameter which is necessary to be determined. The method of determining this parameter will be presented in the next subsection.

Based on actual value of the R ratio and basic value of the endurance stress (threshold stress for $R = -1$), the authors of paper [1] postulate a Wöhler curve $S^{max}_{(R)}(N)$ (compare Eq. (2)) for a given value of R as an exponential function

$$S^{max}_{(R)}(N) = S^{max}_{(R=-1)} + (S_u - S^{max}_{(R)}) \cdot 10^{((ALFAF + (0.5+0.5\cdot R)\cdot AUXR1)\cdot \log(N)^{BETAF})}, \tag{12}$$

where $ALFAF$, $AUXR1$ and $BETAF$ are the fatigue parameters used in numerical code COMET [5]. The method of determining these parameters for specific material and different load scheme (R) will be presented in the next subsection.

Eq. (2) represents "classical" Wöhler approach to fatigue analysis. Eq. (12) is taken from COMET [1,5] and takes into account different constitutive model of fatigue failure. The difference between both models can be seen when comparing Fig. 1 (classical Wöhler) and Fig. 4 (COMET [1,5]). Both models: one starting from Goodman diagram and "classical" Wöhler curves and the other from Ref. [1] had been used in order to validate calculations against experiment.

As it is written at the end of EN 13445 rules description (chapter 18 point 18I) [2], the 'marriage' of stress analysis from FEM and fatigue data is still one of the deficiencies in the current EN 13445. We believe that this paper partially reduces this deficiency.

3. Numerical examples

3.1. Application of Wöhler and Goodman curves dependency for specific material and different load schemes (R)

In this section, an example of determining the values of the fatigue parameters used in numerical code COMET [5] (*ALFAF*, *AUXR*1, *BETAF*, etc.) for some specific material is presented. The fatigue parameters were established in such a way that the Wöhler curve, given by Eq. (12), fits between the points $S^{\max_i}_{(R)}$ and $S^{\max_t}_{(R)}$. The values of $S^{\max_i}_{(R)}$ and $S^{\max_t}_{(R)}$ will be determined from Eqs. (9) and (11). The values of $S^{\max_i}_{(R)}$ and $S^{\max_t}_{(R)}$ and fatigue parameters are used in Sections 4 and 5 for the final calculation of number N of cycles to failure.

To determine the $S^{\max_i}_{(R)}$ and $S^{\max_t}_{(R)}$ from Eq. (9), we have to first calculate the values of $S^{ai}_{(R)}$ and $S^{at}_{(R)}$. The values of factor stresses f^i and f^t (see Eqs. (3) and (4)) necessary to obtain the initial and threshold amplitude stresses (for $R=-1$) were taken from the literature. The initial amplitude stress $S^{ai}_{(R=-1)}$ for $N_i = 1.0\times10^3$ is obtained from Eq. (3) as

$$S^{ai}_{(R=-1)} = S_u \cdot f^i = 520 \cdot 0.9 = 332.8 \text{ MPa}.$$

The value of threshold amplitude stress $S^{at}_{(R=-1)}$ for $N_t = 2.0\times10^6$ is obtained from Eq. (4) as

$$S^{at}_{(R=-1)} = S_u \cdot f^t = 520 \cdot 0.45 = 234.0 \text{ MPa}.$$

For different values of $R \neq -1$, it is necessary to calculate the initial and threshold amplitude stresses from Eq. (10). For example, amplitude stress $S^{ai}_{(R=-0.5)}$ for the given $R=-0.5$ and $N_i = 1.0\times10^3$ is obtained as

$$\begin{aligned} S^{ai}_{(R=-0.5)} &= \frac{S_u S^a_{(R=-1)}(R-1)}{S^a_{(R=-1)}(-1-R)+S_u(R-1)} \\ &= \frac{S_u f^i S_u(R-1)}{f^i S_u(-1-R)+S_u(R-1)} \\ &= \frac{520\cdot0.9\cdot520(-0.5-1)}{0.9\cdot520(-1+0.5)+520(-0.5-1)} \\ &= 360 \text{ MPa}. \end{aligned}$$

The values of the initial and threshold amplitude stress for different R are shown in Table 1 and in Fig. 2.

Mean stress for different values of R calculated from Eq. (7) is shown in Table 2. For example, the initial mean stress for $R=-0.5$ is equal to

$$\begin{aligned} S^{mi}_{(R=-0.5)} &= \frac{S^a(1+R)}{(1-R)} = \frac{S^{ai}_{(R=-0.5)}(1-0.5)}{(1+0.5)} = \frac{360\cdot(1-0.5)}{(1+0.5)} \\ &= 120 \text{ MPa} \end{aligned}$$

Maximal stress $S^{max}_{(R)}$ obtained from Eq. (9) for different values of R is shown in Table 3. For example, maximal initial stress for $R=-0.5$ is equal to

Table 1
Amplitude stress $S^a_{(R)}$ for different values of R obtained from Eq. (10)

N	Amplitude stress S^a				
	$R=-1$	$R=-0.5$	$R=0$	$R=0.5$	$R=1$
1	520	390	260	130	0
1.0×10^3	468	360	246.316	126.486	0
2.0×10^6	234	203.478	161.379	99.574	0
1.0×10^7	234	203.478	161.379	99.574	0

Table 2
Mean stress $S^m_{(R)}$ for different values of R obtained from Eq. (7)

	Mean stress S^m				
R	-1	-0.5	0	0.5	1
$N=1$	0	130	260	390	520
$N=1.0\times10^3$	0	120	246.316	379.459	520
$N=2.0\times10^6$	0	67.826	161.379	298.723	520

Table 3
Maximal stress for different values of R obtained from Eq. (9)

	Maximal stress from Eq. (9)				
R	-1	-0.5	0	0.5	1
$N=1$	520	520	520	520	520
$N=1.0\times10^3$	468	480	492.632	505.946	520
$N=2.0\times10^6$	234	271.3043	322.759	398.298	520
$N=1.0\times10^7$	234	271.3043	322.759	398.298	520

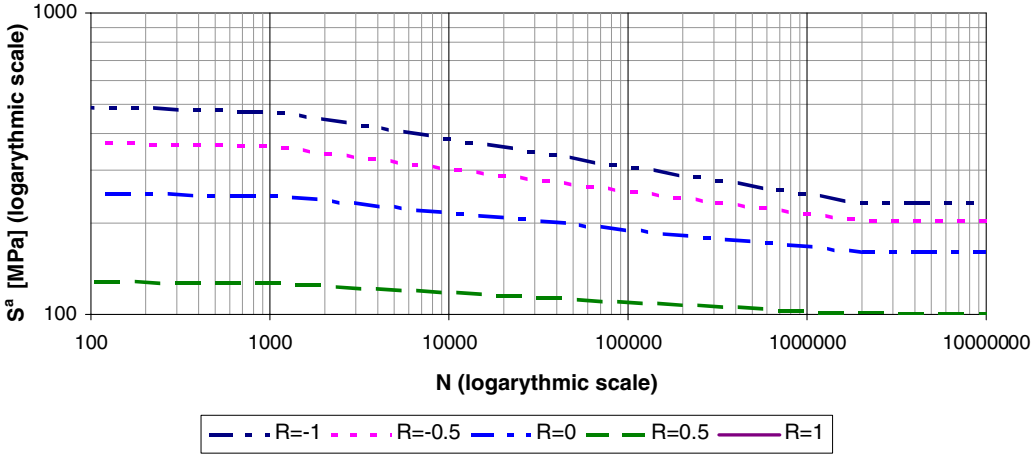

Fig. 2. Amplitude stress for different values of R obtained from Eq. (10).

$$S^{\max_i}_{(R=-0.5)} = S^{ai}_{(R=-0.5)} + S^{mi}_{(R=-0.5)} = 360 + 120 = 480 \text{ MPa}.$$

The same maximal stress $S^{\max}_{(R)}$ can be calculated from Eq. (11) for different values of R and it is shown in Table 4.

For example, value of the initial maximal stress $S^{\max_i}_{(R=-0.5)}$ for given $R = -0.5$ and $N_i = 1.0 \times 10^3$ is obtained as

$$\begin{aligned} S^{\max_i}_{(R=-0.5)} &= S^{\max_i}_{(R=-1)} + (S_u - S^{ai}_{(R=-1)}) \cdot (0.5 + 0.5 \times (-0.5))^{STHR1} \\ &= f^i \cdot S_u + (S_u - f^i \cdot S_u) \cdot (0.5 + 0.5 \times (-0.5))^{STHR1} \\ &= 468 + (520 - 468) \cdot (0.5 + 0.5 \times (-0.5))^{1.7} \\ &= 472.9948 \text{ MPa}. \end{aligned}$$

Value of the threshold maximal stress $S^{\max_t}_{(R=-0.5)}$ for the given $R = -0.5$ and $N_t = 2.0 \times 10^6$ is calculated as

$$\begin{aligned} S^{\max_t}_{(R=-0.5)} &= S^{\max_t}_{(R=-1)} + (S_u - S^{at}_{(R=-1)}) \cdot (0.5 + 0.5 \times (-0.5))^{STHR1} \\ &= f^t \cdot S_u + (S_u - f^t \cdot S_u) \cdot (0.5 + 0.5 \times (-0.5))^{STHR1} \\ &= 234 + (520 - 234) \cdot (0.5 + 0.5 \times (-0.5))^{1.7} \\ &= 261.0934 \text{ MPa}. \end{aligned}$$

Comparison of the results of $S^{\max}_{(R)}$ determined from Eqs. (9) and (11) is shown in Fig. 3. It can be seen that the results determined by both equations are almost the same. There is a small difference between the results for $S^{\max}_{(R=0.5)}$ and $S^{\max}_{(R=-0.5)}$, but it does not exceed 4%.

The method of determining the fatigue parameters used in constructing the Wöhler curve in program COMET is shown below.

Numerical test was performed in order to determine the fatigue parameters *STHR*1, *ALFAF*, *AUXR*1 and *BETAF*. Improperly and properly chosen values of these parameters are shown in Tables 5 and 6, respectively. The fatigue parameters were established in such a way that the Wöhler curve, given by Eq. (12), fits between the points $S^{\max_i}_{(R)}$ and $S^{\max_t}_{(R)}$. Calculations were done for values of initial $S^{\max_i}_{(R=0)} = 484.11$ MPa, $S^{\max_i}_{(R=-1)} = 468$ MPa and threshold maximal stresses $S^{\max_t}_{(R=0)} = 322.6$ MPa, $S^{\max_i}_{(R=-1)} = 234$ MPa determined above. The fatigue parameters have to be set in such a way that for the actual value of R, curve $S^{\max}_{(R)}(N)$ passes through or near the points $S^{\max_i}_{(R)}$ and $S^{\max_t}_{(R)}$ (Fig. 4). The $S^{\max}_{(R)}(N)$ curves for correct values of the

Table 4
Maximal stress for different values of R obtained from Eq. (11)

	Maximal stress from Eq. (11) – sthr1 = 1.7				
R	−1	−0.5	0	0.5	1
$N = 1$	520	520	520	520	520
$N = 1.0 \times 10^3$	468	472.926	484.005	499.887	520
$N = 2.0 \times 10^6$	234	261.093	322.027	409.376	520
$N = 1.0 \times 10^7$	234	261.093	322.027	409.376	520

Table 5
Improperly chosen values of the fatigue parameters

alfaf	0.00095
auxrl	0.0001
sthrl	1
betaf	3

Table 6
Fatigue parameters by COMET

alfaf	0.00095
auxrl	0.0001
sthr1	1.7
betaf	4.1

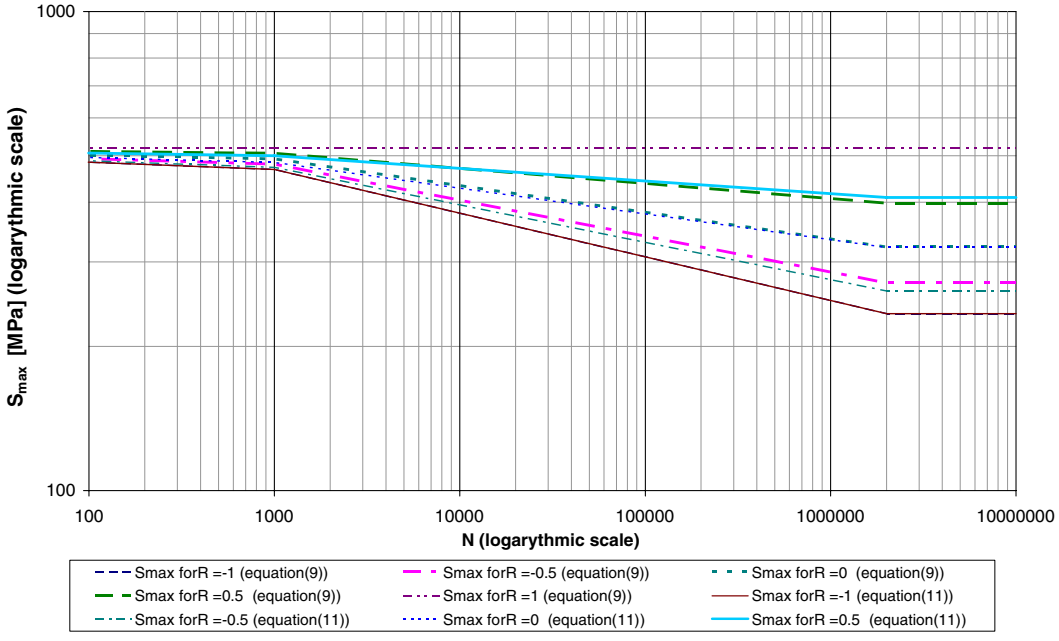

Fig. 3. Maximal stress for different values of R obtained from Eqs. (9) and (11).

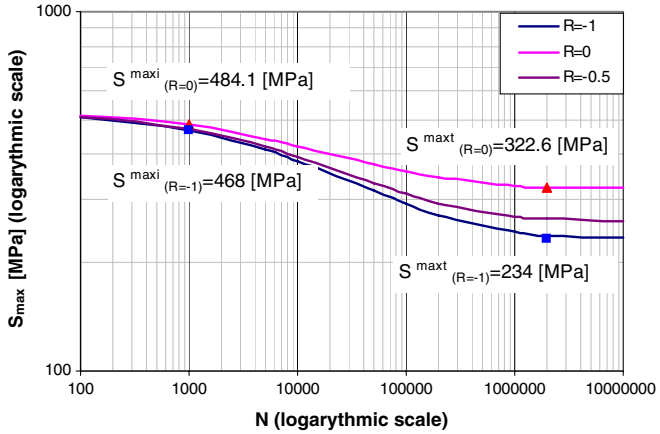

Fig. 4. $S^{\max}_{(R)}(N)$ curves for $R=0$, $R=-0.5$ and $R=-1$. Fatigue parameters are shown in Table 6.

fatigue parameters, for example for $R=-0.5$ (Table 6), are given by equation of type

$$S^{\max}_{(R=-0.5)}(N) = S^{\max_t}_{(R=-0.5)} + (S_u - S^{\max_t}_{(R=-0.5)}) \cdot 10^{((ALFAF+(0.5+0.5\cdot(-0.5))\cdot AUXR1)\cdot\log(N)^{BETAF})} = 261.093 + (520 - 261.093) \cdot 10^{((0.00095+(0.5+0.5\cdot(-0.5))\cdot 0.0001)\cdot\log(N)^{4.1})}.$$

These curves are shown in Fig. 4.

Fatigue parameters that are shown in Table 6 were taken for further calculations.

4. Damage analysis of uniaxially loaded specimen

The test presented was performed in order to compare the results of calculation by program COMET with results of a similar example presented in book [6]. The part of the specimen with circular cross-section was analyzed. The geometrical dimensions are shown in Fig. 5. The length of the specimen is 0.03 m. 9761 tetrahedral finite elements with 4 nodes and 1 gauss point in the element were used to discretize the structure. Material data are as follows: density $\rho = 7800\ \mathrm{kg/m^3}$, Young's modulus $E = 2.1\times10^5$ MPa, Poisson's ratio $v = 0.3$, initial flow stress $R_e = 240$ MPa.

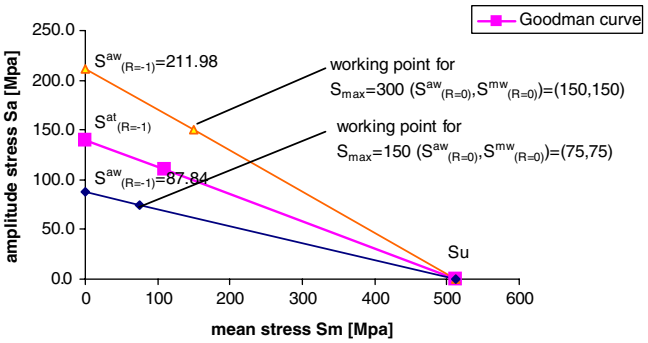

Fig. 6. Goodman diagram for the first load scheme ($R=0$).

Data from book [6]: amplitude threshold stress ($N_t = 2.0\times10^6$) for $R=-1$ and $R=0$ are equal to $S^{at}_{(R=-1)} = 140$ MPa and $S^{at}_{(R=0)} = 110$ MPa, respectively. From Goodman diagram (see Fig. 6) and Eq. (8), we have obtained saturation flow stress $S_u = 513$ MPa.

Two different load schemes were considered: symmetric load for $R=0$ and unsymmetric load for $R=-1$.

4.1. The first load scheme: R = 0

Two values of maximal stress S_{max} were analyzed. In the first case $S_{max} = 300$ MPa, in the second case $S_{max} = 150$ MPa. $S_{min} = 0$ for both cases. Amplitude and mean stress are equal to $S^{aw}_{(R=0)} = S^{mw}_{(R=0)} = 150$ MPa and $S^{aw}_{(R=0)} = S^{mw}_{(R=0)} = 75$ MPa. Working points are indicated in Fig. 6. As it is shown in Fig. 7, for $S_{max} = 300$ MPa the amplitude stress intersects with Wöhler curve. The number of cycles to failure (obtained from Eq. (5)) is equal to $N_w = 1.424\times10^5$. For $S_{max} = 150$ MPa, amplitude stress and Wöhler curve do not intersect. In this case, there is no fatigue for the specimen analyzed. The factor of safety for $S_{max} = 300$ MPa is equal to FOS = 0.733 and for $S_{max} = 150$ MPa it is equal to FOS = 1.466.

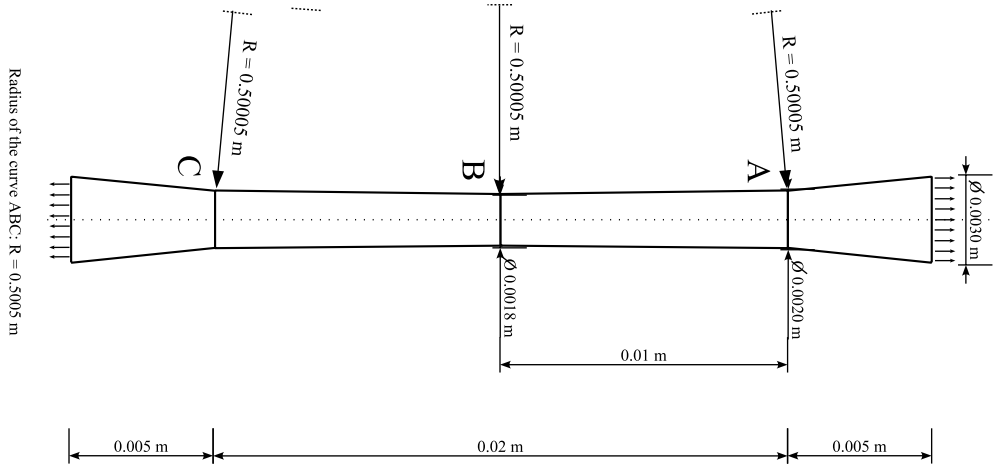

Fig. 5. Specimen.

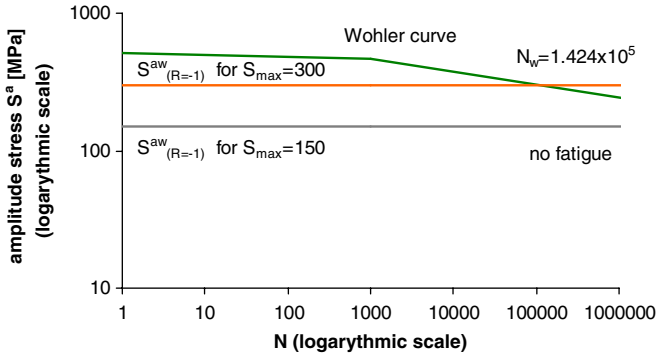

Fig. 7. Wöhler curve and amplitude stress of the working points S^{aw} for the first load scheme $R = 0$.

4.2. The second load scheme: $R = -1/4$ and $R = -1/3$

Two values of S_{max} and S_{min} stresses were analyzed. In the first case, $S_{max} = 160$ MPa and $S_{min} = -40$ MPa. In the second case, $S_{max} = 300$ MPa and $S_{min} = -100$ MPa. Working points are pointed out in Fig. 8.

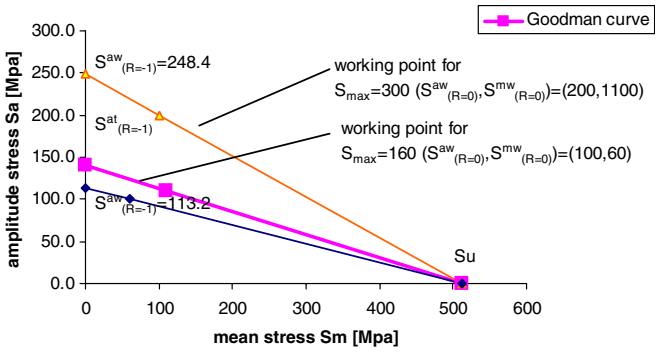

Fig. 8. Goodman diagram for the second load scheme ($R = -1/4$) and ($R = -1/3$).

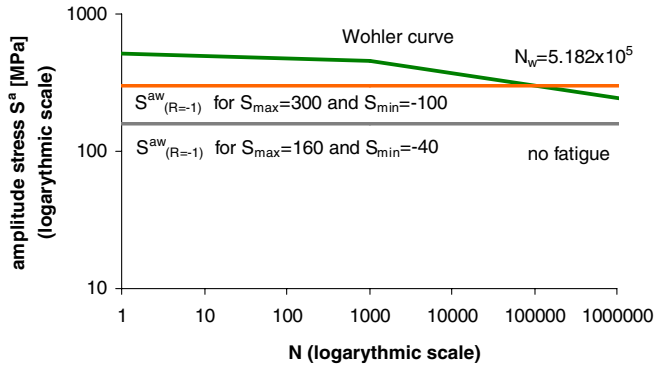

Fig. 9. Wöhler curve and adopted stress amplitude S^{aw}.

As it is shown in Fig. 9, for $S_{max} = 160$ MPa and $S_{min} = -40$ MPa amplitude stress and Wöhler curve do not intersect. In this case, there is no fatigue for the specimen analyzed. Factor of safety for the first case is equal to FOS = 1.203.

For $S_{max} = 300$ MPa and $S_{min} = -100$ MPa, the amplitude stress intersects with Wöhler curve. The number of cycles to failure (obtained from Eq. (5)) is equal to $N_w = 5.182 \times 10^4$. The factor of safety for the second case is equal to FOS = 0.616.

5. Hydraulic cylinder design, oil ports fatigue and possible design modifications

5.1. Fatigue analysis of hydraulic cylinder 1

The cylinder which is shown in Fig. 10 was tested. Critical zones and critical points of cylinders are shown in Fig. 11 (data were obtained from industry). Unfortunately, not precise failure forms and the exact place of microcracks are given. We do not analyze crack mechanism in detail. Stress evaluation was based on single isotropic material model; the material data were the same for weld as for the rest of the cylinder. So the critical points were established just at points where the maximal stress obtained from finite element analysis was observed.

The cylinder has two oil ports. The material of the specimen is steel *St*52. Material data: density $\rho = 7800$ kg/m^3, Young's modulus $E = 2.1 \times 10^5$ MPa, Poisson's ratio $v = 0.3$, initial flow stress $R_e = 350$ MPa, saturation flow stress $S_u = 520$ MPa, saturation hardening law exponent $YEPOW = 45$. Inner pressure 30 ± 0.08 MPa. Ratio p_{min}/p_{max} is equal to 0.

Initial and threshold maximal stress for steel *St*52 and $R = -1$ are equal: $S^{ai}_{(R=-1)} = 0.9 \cdot S_u = 468$ MPa and $S^{at}_{(R=-1)} = 0.45 \cdot S_u = 234$ MPa. Values of fatigue parameters necessary to obtain $S^{max}_{(R)}(N)$–N curve, given by Eq. (12), are shown in Table 6.

Wöhler curve provided by cylinder producer (Roquet SA) takes into account welds, similarly as it is foreseen in European norm EN 13445 (chapter 18 point 18D) shown in figure 18D-1 of EN 13445 [2].

Five critical zones determined in the experiment are shown in Fig. 11. The number of cycles to failure (see Fig. 12) is obtained as intersection of the maximal stress $S^{max_w}_{(R=0)}$ with Wöhler curve. Values of maximal stress in each of the zones and the number of cycles to failure are shown in Table 7.

Number of cycles to failure is obtained by Eq. (5). Values of the maximal stress $S^{max_w}_{(R=0)}$ in each of the zones are shown in

Fig. 10. Geometrical shape of cylinder 1.

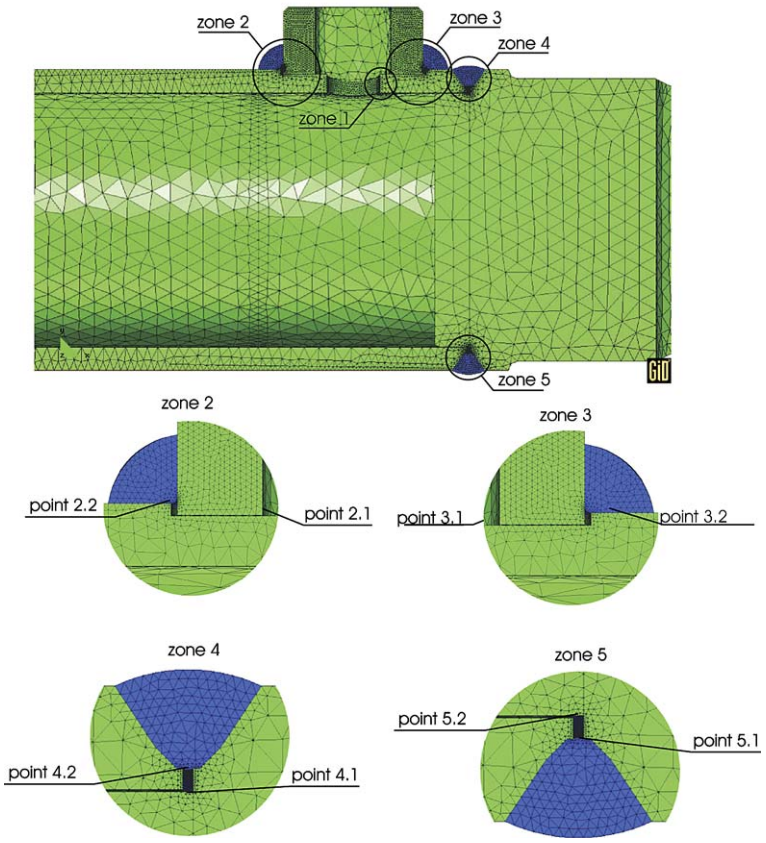

Fig. 11. Critical zones and critical points in cylinder 1.

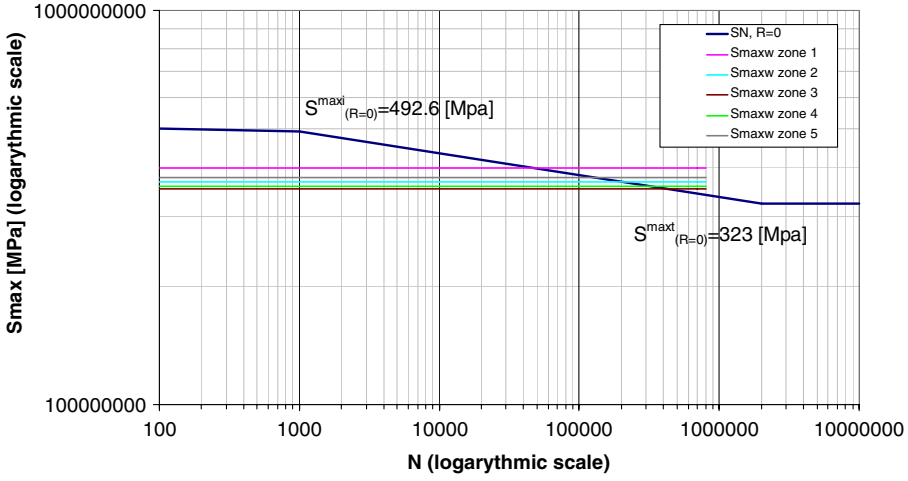

Fig. 12. Behavior of the Wöhler curve and values of maximal stress $S^{\max_w}$ in critical zones for cylinder 1.

the second row in Table 7. For each of the zones, three values of the number of cycles to failure were determined: N_1, N_2, N_3. N_1 was obtained as a function of the amplitude stress by

$$N_1 = 10^{\frac{\log(S^{aw}_{(R=-1)})\log(N_i)-\log(S^{aw}_{(R=-1)})\log(N_t)+\log(S^{ai}_{(R=-1)})\log(N_t)-\log(S^{at}_{(R=-1)})\log(N_i)}{\log(S^{ai}_{(R=-1)})-\log(S^{at}_{(R=-1)})}} \quad (13)$$

substituting values of the threshold and initial maximal stress from the first row of Table 8.

For $N_1 : S^{at}_{(R=-1)} = 0.9S_u$ and $S^{ai}_{(R=-1)} = 0.45S_u$. N_2 was determined as a function of the maximal stress by

$$N_2 = 10^{\frac{\log(S^{maxw}_{(R)})\log(N_i)-\log(S^{maxw}_{(R)})\log(N_t)+\log(S^{max_i}_{(R)})\log(N_t)-\log(S^{max_t}_{(R)})\log(N_i)}{\log(S^{max_i}_{(R)})-\log(S^{max_t}_{(R)})}} \quad (14)$$

Table 7
Number of cycles to failure in critical zones of cylinder 1

	Zone 1	Zone 2 (point 2.2)	Zone 3 (point 3.2)	Zone 4 (point 4.2)	Zone 5 (point 5.1)
$S^{\max_w}_{R=0}$ (MPa)	399.13	367	352.1	357.38	376.76
$S^{aw}_{R=0}$ (MPa)	199.57	183.50	176.05	178.69	188.38
$S^{mw}_{R=0}$ (MPa)	199.57	183.50	176.05	178.69	188.38
$S^{aw}_{R=1}$ (MPa)	323.85	283.57	266.16	272.24	295.39
Number of cycles to failure N_1, from Eq. (13)	56,670	243,300	486,900	380,300	155,400
Number of cycles to failure N_2 from Eq. (14)	36,480	174,600	377,900	286,500	107,000
Number of cycles to failure N_3 from Eq. (14)	43,960	198,700	418,300	320,300	124,000
FOS	0.89	0.879	0.917	0.903	0.857

Table 8
Initial and threshold stresses necessary for calculating N_1, N_2 and N_3

$S^{ai}_{(R=-1)} = 0.9 * S_u = 468$	$S^{at}_{(R=1)} = 0.45 * S_u = 234$	Initial and threshold stress are obtained by Eqs. (3) and (4)
$S^{\max_i}_{(R=0)} = 484.116$	$S^{\max_t}_{(R=0)} = 322.027$	initial and threshold stress are obtained by Eq. (11)
$S^{\max_i}_{(R=0)} = 492.63$	$S^{\max_t}_{(R=0)} = 322.758$	Initial and threshold stress are obtained by Eq. (9)

substituting values of the threshold and initial maximal stress determined from Eq. (11) shown in the second row of Table 8.

N_3 was determined by Eq. (14). The values of the threshold and initial maximal stress were determined from Eq. (9). The determined values of the threshold and initial maximal stress are also shown in the third row of Table 8.

For N_2 the initial and threshold stress were taken from the third row of Table 4. For N_3 the initial and threshold stress were taken from the third row of Table 3.

The behavior of $f_{\mathrm{red}(R)}(N)$ is shown in Fig. 13. Curves $f_{\mathrm{red}(R)}(N)$, Wöhler and maximal stress intersected for 2.0×10^5 number of cycles. Values of the amplitude and mean stresses for working points in each zone are shown in Fig. 14. All working points are located above the Goodman diagram. Goodman diagram is shown as a blue line in Fig. 14. This diagram determines the area where fatigue crack may occur.

The number of cycles to failure in zone *5* (see Fig. 11) is equal to about $N_1 = 1.55 \times 10^5$. The difference between the results obtained by the experiment and the numerical test does not exceed 9%.

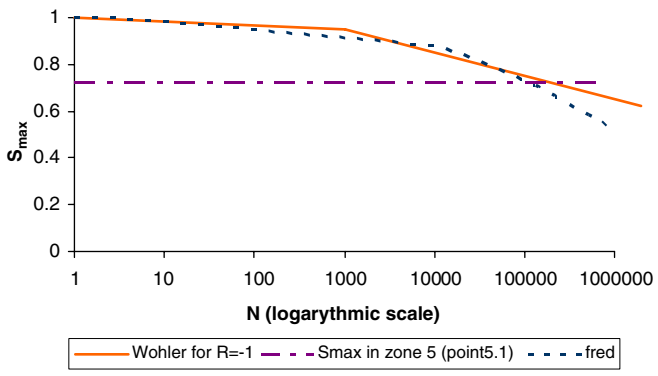

Fig. 13. Behavior of the Wöhler and $f_{\mathrm{red}}(N)$ curves in critical zone 5 for cylinder 1.

The largest value of stress appears in zone 1, then next in zone 5 (point 5.1) and successively in zone 2 (point 2.1), and in zones 4 and 3 (points 4.1 and 3.1) (see Fig. 11). The location where fatigue crack appears first are points 5.1 and 2.1. This fact was confirmed in the real experiment.

In the case when the washer or glue is used between the oil port and the cylinder (see Fig. 19) the largest value of stress appears also in zone 1. Unfortunately, the results of real experiment do not confirm this fact. Consecutive places of fatigue crack propagation are points 2.2, 3.2, 4.2, and 5.2 (different points than in the former case). Significant improvement was archived in zone 5 where fatigue strength increased and the number of cycles was bigger for about 1.0×10^5 cycles. In zones 2, 3 and 4, there was a slight improvement in the value of fatigue strength.

5.2. Fatigue analysis of hydraulic cylinder 2

The part of hydraulic cylinder was analyzed. The geometrical shape is shown in Fig. 15. The cylinder has two oil ports.

The material of the cylinder is steel *St*52. Material data are the same as those in the previous example. The inner pressure is equal to 10 MPa. Ratio $p_{\min}/p_{\max}$ is equal to 0. The initial and threshold stress for steel *St*52 and $R = 0$ are taken from the previous example. The values of fatigue parameters are shown in Table 6.

Deformations and stress redistribution in connection zone caused by oil penetration and shear forces inside the oil tube are shown in Fig. 16.

Values of the maximal stresses (for $R = 0$), amplitude and mean stresses for $R = 0$ and $R = -1$, and number of cycles to failure in each zone are shown in Table 9. Values

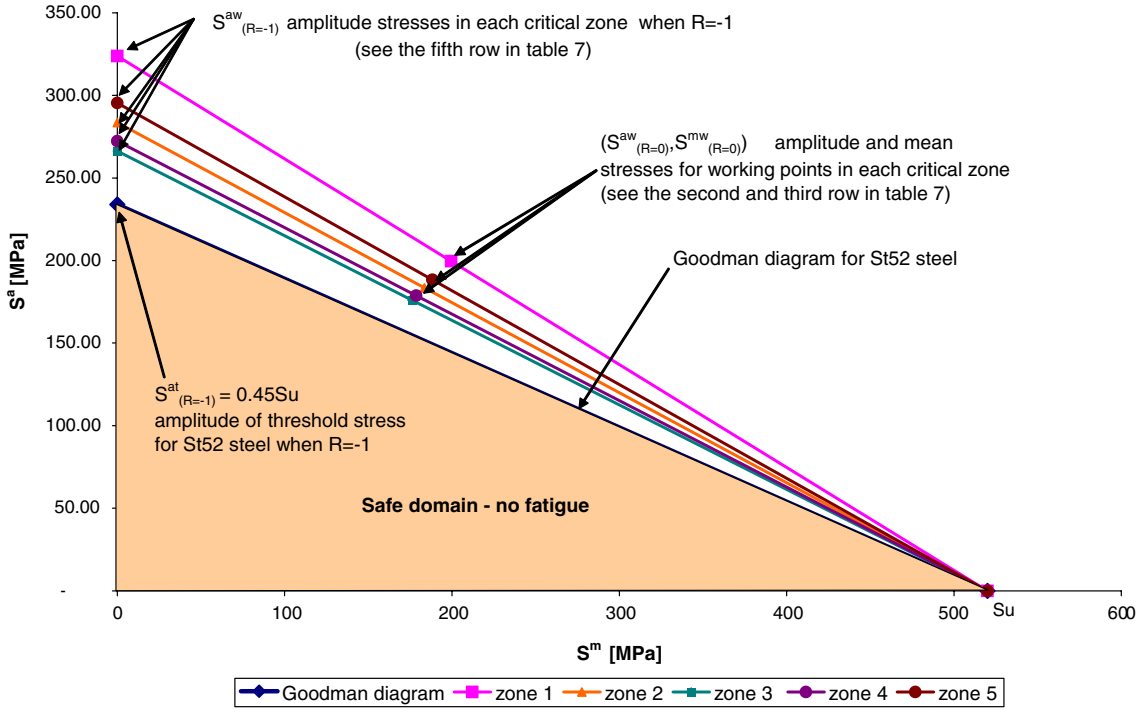

Fig. 14. Goodman diagram and working points for cylinder 1, for different critical zones.

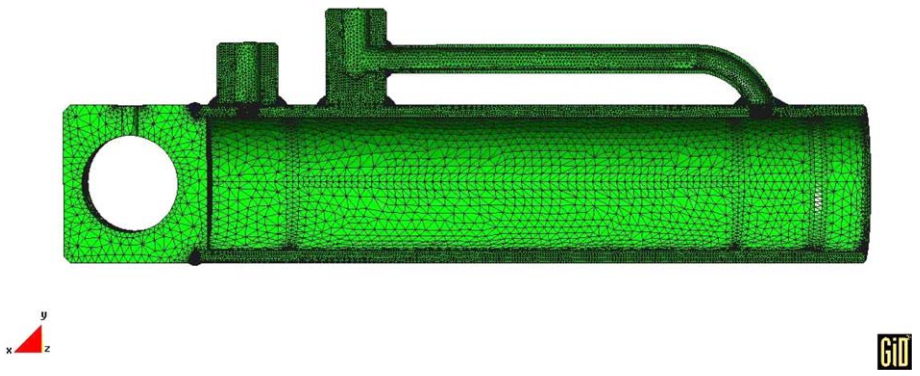

Fig. 15. Geometrical shape of cylinder 2.

of the maximal stresses in zone 1 and zone 5 are almost the same. These two working points (zone 1 and zone 5) are located above the Goodman diagram, the other points are lying below the Goodman diagram in a safe area (see Fig. 17). Fatigue crack will appear in zones 1 and 5. Cracks will not appear in other zones. The number of cycles to failure in zone 1 and zone 5 obtained as intersection of the maximal stress with Wöhler curve are shown in Table 9 and in Fig. 18.

5.3. Fatigue analysis of hydraulic cylinder 1 with resistant material in oil ports and cup

The part of hydraulic cylinder was analyzed. The geometrical shape and material data are the same as those in

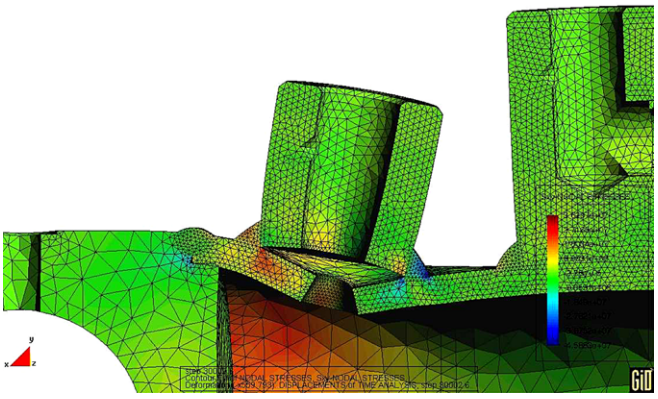

Fig. 16. Deformations and stress redistribution in connection zone caused by oil penetration and shear forces inside the oil tube of cylinder 2.

Table 9
The number of cycles to failure in critical zones of cylinder 2

	Zone 1	Zone 2 (point 2.2)	Zone 3 (point 3.2)	Zone 4 (point 4.2)	Zone 5 (point 5.1)
$S^{max_w}_{(R=0)}$ (MPa)	350.00	219.00	255.00	130.00	352.00
$S^{aw}_{(R=0)}$ (MPa)	175.19	109.34	127.25	65.25	175.84
$S^{mw}_{(R=0)}$ (MPa)	175.19	109.34	127.25	65.25	175.84
$S^{aw}_{(R=-1)}$ (MPa)	254.20	138.45	168.48	74.61	265.68
Number of cycles to failure N_1, from Eq. (13)	528,000	No fatigue	No fatigue	No fatigue	497,000
Number of cycles to failure N_2 from Eq. (14)	414,000	No fatigue	No fatigue	No fatigue	387,000
Number of cycles to failure N_3 from Eq. (14)	457,000	No fatigue	No fatigue	No fatigue	428,000
FOS	0.921	1.476	1.268	2.473	0.918

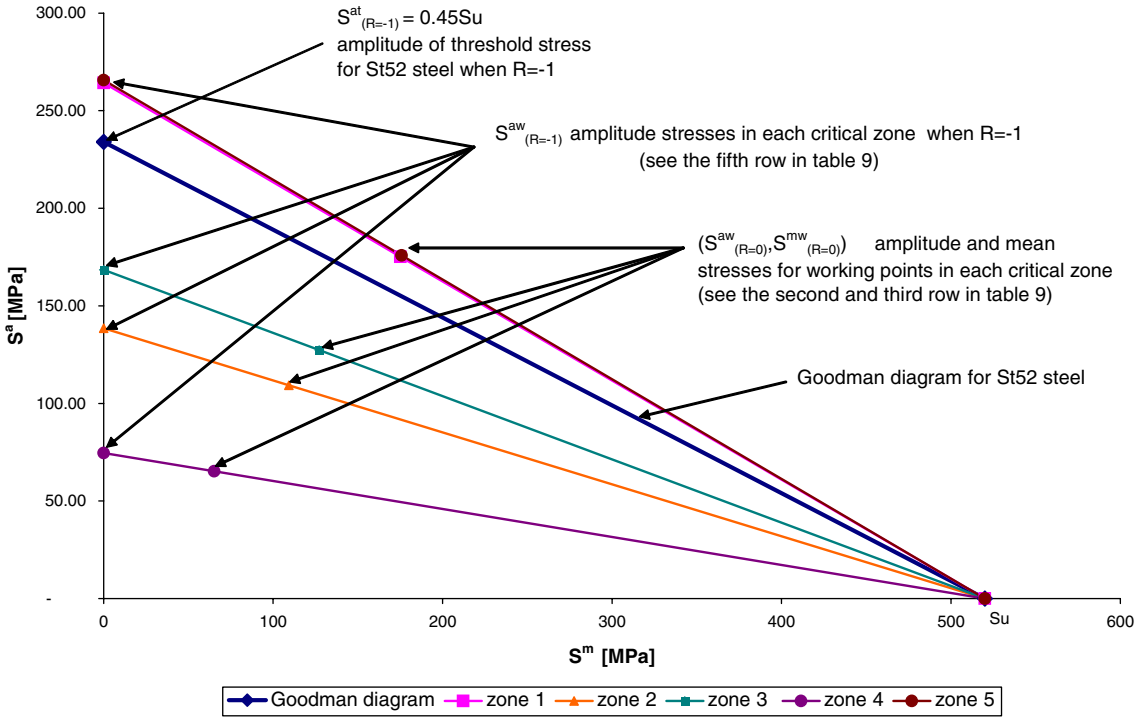

Fig. 17. Goodman diagram and working points in critical zones for cylinder 2.

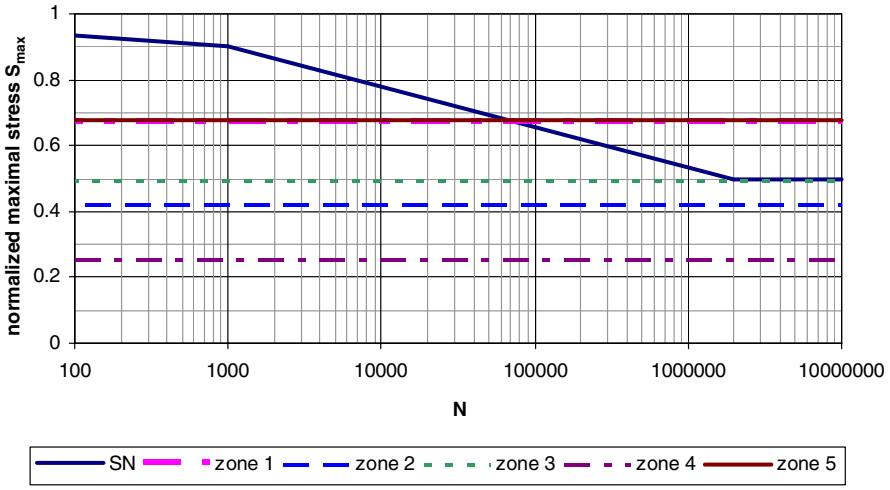

Fig. 18. Behavior of the Wöhler curve and values of maximal stress $S^{max_w}_{(R=0)}$ in critical zones for cylinder 2.

the example mentioned in Section 5.1. The authors propose a modification of the oil ports area by introducing the washer or glue as it is shown in Fig. 19. The cylinder has two oil ports with washers.

The number of cycles to failure in each zone obtained as intersection of the maximal stress with Wöhler curve are shown in Table 10.

Deformations and von Mises stress redistribution in connection zone are shown in Fig. 20.

Behavior of the Wöhler curve and values of maximal stress $S^{\max_w}_{(R=0)}$ in critical zones are shown in Fig. 21.

The fatigue in zone 2 appears later if we use a washer between the oil port and the cylinder (see Fig. 19). The value of maximal stress is lower than in the case when there is no modification between the oil port and the cylinder surface.

The set of indexes used in this paper is presented in Table 11.

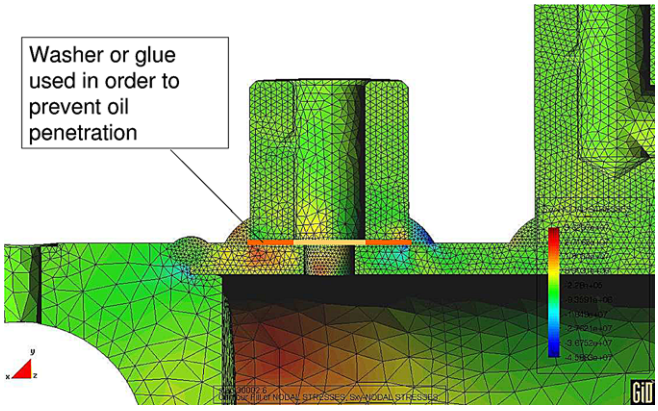

Fig. 19. Washer or glue used in order to prevent oil penetration.

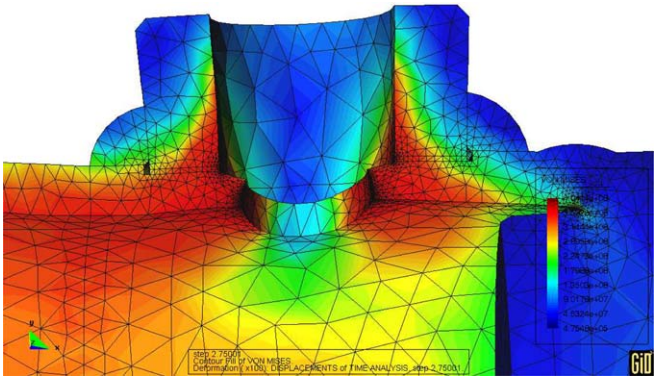

Fig. 20. Deformations and stress redistribution in connection zone with washer used in order to prevent oil penetration in cylinder 1.

Table 10
The number of cycles to failure in critical zones of cylinder 1 with washer

	Zone 1	Zone 2 (point 2.1)	Zone 3 (point 3.1)	Zone 4 (point 4.1)	Zone 5 (point 5.2)
$S^{\max_w}_{(R=0)}$ (MPa)	398.17	365.66	360.42	359.14	357.11
$S^{aw}_{(R=0)}$ (MPa)	199.08	182.83	180.21	179.57	178.55
$S^{mw}_{(R=0)}$ (MPa)	199.57	183.50	176.05	178.69	188.38
$S^{aw}_{(R=-1)}$ (MPa)	323.07	282.53	272.45	273.59	279.99
Number of cycles to failure N_1, from Eq. (13)	59,160	258,700	330,000	350,300	385,200
Number of cycles to failure N_2 from Eq. (14)	38,160	186,800	244,600	261,400	290,600
Number of cycles to failure N_3 from Eq. (14)	45,910	212,200	275,100	293,200	324,700
FOS	0.811	0.883	0.896	0.899	0.904

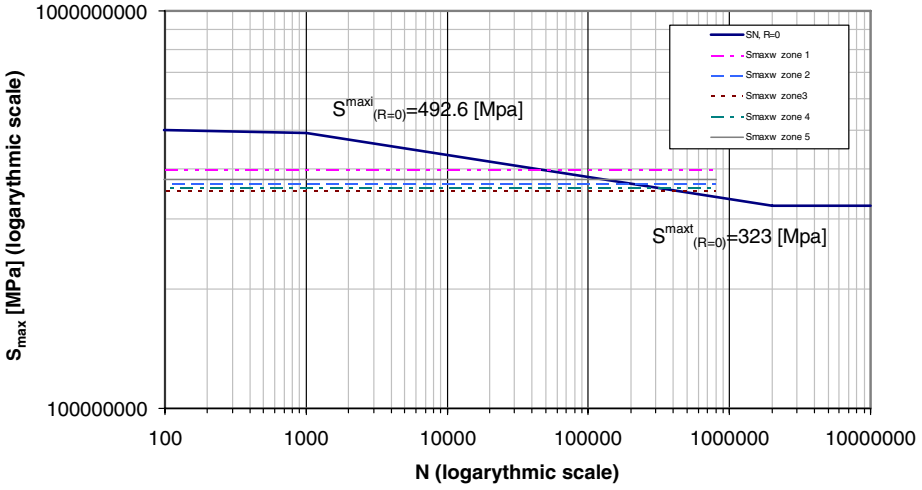

Fig. 21. Behavior of the Wöhler curve and values of maximal stress $S^{\max_w}_{(R=0)}$ in critical zones for cylinder 1.

Table 11
Table of indexes

Report	COMET or Roquet	Explanation
ρ	*DENSI*	Density
E	*YOUNG*	Young's modulus
v	*POISS*	Poisson's ratio
σ_0	*YEINI*	Initial flow stress
	YEFIN	Saturation flow stress
	YEPOW	Saturation hardening law exponent
p		Inner pressure
$p_{\min}$		Minimal values of inner pressure
$p_{\max}$		Maximal values of inner pressure
p_{m}		Values of the mean of inner pressure
p_{a}		Values of amplitude of the inner pressure
$R = \frac{p_{\min}}{p_{\max}}$		Ratio between the $p_{\max}$ and $p_{\max}$
N		Number of cycles
$N_{\mathrm{t}}, N_{\mathrm{i}}$		Number of cycles $N_{\mathrm{t}} = 2 \times 10^6$ and $N_{\mathrm{i}} = 1 \times 10^3$
N_1, N_2, N_3		Number of cycles to failure calculated by Eqs. (13) and (14)
S_{u}		Ultimate stress
f^{i}		Factor of stress corresponding to $N_{\mathrm{i}} = 1 \times 10^3$ of cycles
f^{t}		Factor of stress corresponding to $N_{\mathrm{t}} = 2 \times 10^6$ of cycles
$S^{\mathrm{at}}_{(R)}, S^{\mathrm{ai}}_{(R)}$		Amplitude threshold ($N_{\mathrm{t}} = 2 \times 10^6$) and initial stress ($N_{\mathrm{i}} = 1 \times 10^3$) for the given R
$S^{\mathrm{at}}_{(R=-1)}, S^{\mathrm{ai}}_{(R=-1)}$		Amplitude threshold and initial stress ($N_{\mathrm{i}} = 1 \times 10^3$) for $R = -1$
$S^{\mathrm{aw}}_{(R)}, S^{\mathrm{mw}}_{(R)}$		Amplitude and mean stress for the working point N_{w} for the given R
$S^{\max}_{(R)}(N)$		Wöhler curve for the given R
$S^{\max}_{(R)}$		Maximal stress for the given R
$S^{\max_{\mathrm{t}}}_{(R)}, S^{\max_{\mathrm{i}}}_{(R)}$		Maximal threshold ($N_{\mathrm{t}} = 2 \times 10^6$) and initial stress ($N_{\mathrm{i}} = 1 \times 10^3$) for the given R
$S^{\max_{\mathrm{w}}}_{(R)}$		Maximal stress for working point for the given R
FOS		Factor of safety

6. Conclusions

In order to solve the crack problem in oil port area, we propose to use the washer made from temperature resistant material or glue in order to fill up the gap between the oil port and the cylinder surface (see Fig. 19). Such washer or glue will prevent oil penetration into the above mentioned gap, thus eliminating the possibility of promotive fatigue crack in neighboring welds.

Life expectancy are values of the moment absolutely theoretical, and pending of the adjustment of the model and experimental validation.

Acknowledgements

"PROHIPP" project is partially funded by the E.C. inside the sixth framework programme, priority 3 NMP FP62002-NMP-2-SME, Research area 3.4.3.1.5: Support to the development of new knowledge based added value products and services in traditionally less RTD intensive industries.

We thank the financial contribution of the E.C. and we state that the article reflects only the personal opinion of the authors.

The authors are indebted to Roquet SA and to CIMNE for providing experimental data and numerical code COMET used in these calculations.

References

[1] Oller S, Salomon O, Onate E. A continuum mechanics model for mechanical fatigue analysis. Comput Mater Sci 2005;32(2): 175–95.
[2] European Norm EN 13445. Unifired pressure vessels, chapter 18: detailed assessment of fatigue life. Available from: http://www.unm.fr/en/general/en13445/default.htm.
[3] Zahavi E, Torbilo V. Fatigue design. Life expectancy of machine parts. Boca Rato, New York, London, Tokyo: Solomon Press Book; 1996.
[4] Frost N, Marsh K, Pook L. Metal fatigue. Mineola (NY): Dover; 1999.
[5] Cervera M, Agelet de Saracibar C, Chiumenti M. COMET coupled mechanical and thermal analysis, data input manual. Barcelona: International Center for Numerical Method in Engineering (CIMNE); 2002.
[6] Brzoska Z. Wytrzymałość materiałów (Strength of materials). Warsaw: PWN; 1983.